NACA RM L54L31a

NACA

RESEARCH MEMORANDUM

AN EXPERIMENTAL STUDY OF A METHOD OF DESIGNING THE SWEPTBACK-WING—FUSELAGE JUNCTURE FOR REDUCING THE DRAG AT TRANSONIC SPEEDS

By Robert R. Howell and Albert L. Braslow

Langley Aeronautical Laboratory
Langley Field, Va.

NATIONAL ADVISORY COMMITTEE
FOR AERONAUTICS

WASHINGTON

March 23, 1955
Declassified October 31, 1958

NATIONAL ADVISORY COMMITTEE FOR AERONAUTICS

RESEARCH MEMORANDUM

AN EXPERIMENTAL STUDY OF A METHOD OF DESIGNING THE SWEPTBACK-WING—FUSELAGE JUNCTURE FOR REDUCING THE DRAG AT TRANSONIC SPEEDS

By Robert R. Howell and Albert L. Braslow

SUMMARY

An investigation has been made in the Langley transonic blowdown tunnel at Mach numbers between 0.84 and 1.32 at an angle of attack of 0° to determine the pressure-drag reductions attainable on a sweptback-wing—fuselage configuration by means of various methods of body modification. The general configuration tested consisted of a 45° sweptback wing of aspect ratio 4 in combination with a fineness-ratio-6.7 body. The results indicate that the pressure drag of a practical sweptback-wing—body configuration depends upon the body cross-sectional shape as well as upon the longitudinal distribution of cross-sectional area.

Pressure-drag reductions greater than those obtained by an axisymmetrical indentation of the fuselage in accordance with the principles of the transonic area rule were obtained at Mach numbers between 1.0 and 1.13 with a configuration having the same longitudinal distribution of area and a localized fuselage shaping in the wing-root juncture in accordance with the natural streamline flow over an infinite sweptback wing. Significant reductions in the pressure drag of the basic configuration were also obtained by contouring the fuselage to approximate the natural streamline flow in the region of the wing-root juncture without regard for the area development.

INTRODUCTION

Modification to fuselages of wing-fuselage combinations in accordance with the principles of the transonic area rule (ref. 1) has been shown in numerous experimental investigations to be a most effective means of reducing the pressure drag in the transonic speed range. Strict theoretical verification of the area rule, however, has been accomplished only through inclusion of many qualifying assumptions in the derivation of the rule. (See ref. 2.) It is obvious that, in actuality, fulfillment

of these assumed conditions is not possible so that it appears logical that more than just the longitudinal distribution of cross-sectional area is involved in the pressure-drag characteristics of wing-body combinations. It seems likely, then, that it should be possible to obtain further pressure-drag reductions by considering, in addition to the overall longitudinal area distribution, details of local flow conditions.

A region in which local flow conditions seem to be especially important is in the wing-fuselage juncture. Experimental results in references 3 to 7 have indicated that it is possible to decrease the constricting effects of a fuselage on the flow in the wing root with resultant pressure-drag reductions at supercritical speeds by means of fuselage contouring in the region of the wing root; the contouring methods used were in accordance with the theoretical concepts of references 8 and 9. The present investigation was undertaken, therefore, to determine whether such localized fuselage contouring in the region of the root of a sweptback wing could be combined with the area-rule body indentation to afford pressure-drag reductions greater than those attainable with the area-rule indentation alone. The localized fuselage contour used in the present investigation was based on the concept of reference 8 in that the fuselage sides were modified to approximate the natural streamline curvature over an infinite sweptback wing. Tests were also made to determine the pressure-drag reductions attainable by means of this streamline contouring alone.

The investigation was made in the Langley transonic blowdown tunnel of a wing-body combination having a 45° sweptback wing of aspect ratio 4, taper ratio 0.6, and NACA 65A006 airfoil sections in the stream direction. The models were tested at an angle of attack of 0° through a range of Mach number from 0.84 to 1.32 at a Reynolds number of approximately 2.7×10^6 based on the wing mean aerodynamic chord.

SYMBOLS

A_b area of base

C_{D_T} total drag coefficient, $\frac{\text{Measured drag}}{q_o S}$

C_{D_b} base drag coefficient, $-\left(p_b - p_o\right)\frac{A_b}{q_o S}$

C_D net drag coefficient, $C_{D_T} - C_{D_b}$

ΔC_D incremental net drag coefficient

p_b measured base pressure

p_o free-stream static pressure

M_o free-stream Mach number

q_o free-stream dynamic pressure, $0.7p_oM_o^2$

S total plan-form area of wing, 12.960 sq. in.

APPARATUS

The investigation was made in the Langley transonic blowdown tunnel which has an octagonal slotted test section measuring 26 inches between flats. The models were mounted on an internal electrical strain-gage balance supported by a sting at an angle of attack of 0°. The angle was set with a sensitive inclinometer and was unchanged for all the tests. The force data were recorded by photographing self-balancing potentiometers.

The model base pressure was measured with an open-end tube inserted through the center of the sting into an open section of the balance. The pressure so measured was the average static pressure in the annular opening around the sting in the plane of the model base. The base pressure as well as the pressures required for determination of Mach number, dynamic pressure, and Reynolds number were recorded by a quick-response flight-type pressure recorder.

MODELS

Photographs of the configurations tested are presented as figure 1 and the ordinates are tabulated in table I.

The basic wing-fuselage model consisted of a sweptback wing of aspect ratio 4, taper ratio 0.6, 45° quarter-chord sweep, and NACA 65A006 airfoil sections in the stream direction mounted in a midwing position on a fuselage of fineness ratio 6.67 (fig. 2). The fuselage was composed of a fineness-ratio-3 nose section defined by the relation $r \propto x^{1/2}$, a cylindrical center section, and a truncated conic tail section with a slope of 4.5°. Both the nose section and the tail section were faired to the cylindrical center section to provide a smooth surface contour. Body ordinates are presented in table I(a).

One of the fuselage models investigated was indented according to the area-rule principle of reference 1. As in reference 1, the fuselage was symmetrically indented so that the longitudinal area distribution of the wing-fuselage configuration was the same as the area distribution of the basic fuselage alone. Ordinates for this configuration are also presented in table I(a), and a sketch of the configuration is presented in figure 2.

The second modified fuselage model investigated was designed to combine the longitudinal area development required from the area-rule concept with a localized fuselage contouring in the region of the wing root. The wing-fuselage-juncture contouring used was similar to that investigated in reference 7 and is based on the theoretical concept of reference 8, which is that the disturbances induced over the inboard sections of the wing by the presence of the fuselage can be eliminated if the fuselage is contoured according to the lateral streamline pattern that would exist over an infinite sweptback wing. (See refs. 10 and 11.)

This fuselage model was contoured first so as to approximate the lateral streamline curvature at the wing surface that would exist at a free-stream Mach number of 1.02 if the wing were of infinite span. The following procedure was used to obtain this approximation. The components of the local velocities normal to the wing leading edge were obtained through the use of the normal component of the free-stream velocity and unpublished high-subsonic-speed experimental pressure-distribution data for an NACA 65A009 airfoil section. (The airfoil section normal to the model wing leading edge was 8.7-percent-chord thick and was slightly different in section contour.) The slope of the resultant velocity at each point along the chord was then obtained by combining the local normal velocity component with the component of the free-stream velocity tangent to the leading edge. These slopes were multiplied by incremental distances along the chord to obtain incremental lateral displacements which were summed progressively from the intersection of the wing leading edge with the fuselage to obtain the streamline path over the surface of the swept-back wing. The side of the fuselage was indented with a plane cut normal to the wing-chord plane such that the intersection of the wing and fuselage formed the calculated streamline path between the wing leading and trailing edges. Inasmuch as the indentation began at the intersection of the wing leading edge and body and was only two-dimensional in nature, it is obvious that the fuselage contouring was only an approximation of the actual streamline contour over an infinite sweptback wing (ref. 8). Volume was then removed from the top and bottom of the fuselage as required to allow the area development of the fuselage to be identical with that of the area-rule-indented fuselage. The design ordinates of this body are presented in table I(b).

A third modification to the basic fuselage consisted of the fuselage streamline contouring in the wing-fuselage juncture without regard for

longitudinal area development. Ordinates for this body modification are presented in table I(a) with a sketch showing a typical cross section. A sketch of the configuration is presented in figure 2.

A comparison of the longitudinal area development for the configurations investigated is given in figure 3. Photographs of the four wing-body configurations tested are presented as figure 1. The photographs in figures 1(a), (b), and (c) were taken after the testing was complete when contrasting paint was used on the wing and fuselage in an effort to define more clearly the fuselage shapes in the region of the wing-root juncture.

TESTS

The tests were made through a range of Mach number from 0.84 to 1.32 at Reynolds numbers ranging from 2.57×10^6 to 2.95×10^6 based on the wing mean aerodynamic chord. For the ratio of model to tunnel size used, reference 12 indicates negligible tunnel-wall interference at subsonic speeds. At supersonic speeds, the data are also equivalent to free-air values except for a range of Mach number where wall-reflected disturbances interfere with the measurements. Based on the measurements of base pressure and previous experience on models of similar size, it appears that, for the fuselage alone, the results would be affected by the wall reflections between Mach numbers of 1.02 and 1.13. The interference range is increased, however, to a Mach number of about 1.18 for the wing-fuselage configurations due to intersection of the wing tip by the reflected disturbances. The increment in drag coefficient between the different wing-fuselage configurations should be valid, however, at Mach numbers of 1.13 and greater inasmuch as the wing-tip interference should be the same for all configurations.

The base drag coefficient was obtained from the difference between the measured base pressure and free-stream static pressure and was algebraically subtracted from the measured total drag coefficient to obtain the net drag coefficient. The estimated maximum errors in total and base drag coefficients are ± 0.0007 and ± 0.0005, respectively. The general level of accuracy is believed to be better than these limiting estimates.

RESULTS AND DISCUSSION

The basic drag characteristics at an angle of attack of 0° of the four wing-body configurations investigated are presented in figure 4 as a function of free-stream Mach number. Presented are the total drag coefficient, base drag coefficient, and net drag coefficient all based

on the total wing area. The net drag coefficients for the four wing-body combinations are replotted in figure 5 for comparison and the variations with Mach number of the increments in net drag coefficient above a Mach number of 0.85 are presented in figure 6. The latter plot, of course, is representative of the variation of pressure-drag coefficient with Mach number of the wing-fuselage configuration and indicates the usual reductions in pressure-drag coefficient due to the area-rule indentation throughout the transonic speed range.

The reduction in drag coefficient indicated at subsonic speeds in figure 5 between the combination contouring and the other configurations is greater than can be accounted for by experimental accuracy and is possibly due to unnoticed differences in model surface condition. It does not appear logical that the reduction in drag coefficient due to surface condition at the supersonic Mach numbers would be greater than that measured at subsonic speeds so that the reduction in pressure-drag coefficient due to the combination contouring should be at least as great as that indicated in figure 6.

It can be seen in figure 6 that the combination of the two concepts of body contouring reduced the pressure-drag coefficient as compared with that of the area-rule-indented configuration by 0.0015 (13 percent) at a Mach number of 1.0 and a maximum of 0.0030 (about 16 percent) in a range of Mach number near 1.02, the design Mach number for the streamline contouring. These results substantiate the idea that the pressure drag of sweptback-wing—body combinations depends upon the fuselage cross-sectional shape as well as upon the longitudinal distribution of cross-sectional area.

An increase in Mach number above the design value is indicated in figure 6 to decrease the effectiveness of combining the two contouring concepts. Larger reductions in pressure drag at these higher test Mach numbers may be possible with the use of a fuselage indented in accordance with the supersonic area rule (ref. 13) in combination with a streamline contouring on the side of the body designed for the same supersonic Mach number. Further research is needed on configurations of this type as well as on the effectiveness of the combined area rule and streamline contouring at lifting conditions.

The data in figure 6 also indicate appreciable reductions in pressure-drag coefficient of the basic configuration due to the streamline fuselage contouring alone at Mach numbers from force break to 1.3, the maximum of the tests. This result is similar to that obtained by Pepper (ref. 7) on a sweptback wing-body configuration of appreciably different proportions than the one tested in the present investigation; this indicates that the gains to be expected from streamline contouring may not be sensitive to detailed differences in the configuration of practical sweptback-wing—body combinations. In comparing the drag reduction

obtained by streamline contouring with that obtained from application of the transonic area rule, it is seen that, for the present case, both drag reductions were very nearly the same at a Mach number of 1.0 and at Mach numbers greater than 1.1. A maximum difference in pressure-drag coefficient of about 0.0025 occurred at Mach numbers of 0.97 and 1.03. It is of interest to note in figure 3 that the volume removed from the fuselage by the streamline contouring was less than one-third that removed by application of the transonic area-rule concept. The comparison obtained for the configuration investigated, however, should not be assumed to be universal inasmuch as the magnitude of pressure-drag reduction attainable with either the area-rule indentation or streamline contouring will depend on the degree to which the configuration departs from the limitations of the area rule. For example, for a sweptback-wing—body combination which approaches a theoretically slender configuration, the pressure drag would depend upon only the longitudinal area development; whereas, for a combination which departs appreciably from a theoretically slender configuration, the pressure drag would depend upon localized flow conditions as well as upon the area distribution.

CONCLUDING REMARKS

An investigation has been made in the Langley transonic blowdown tunnel at Mach numbers between 0.84 and 1.32 at an angle of attack of 0° to determine the pressure-drag reductions attainable on a sweptback-wing—fuselage configuration by means of various methods of body modification. The general configuration tested consisted of a 45° sweptback wing of aspect ratio 4 in combination with a fineness-ratio-6.7 body. The results indicate that the pressure drag of a practical sweptback-wing—body configuration depends upon the body cross-sectional shape as well as upon the longitudinal distribution of cross-sectional area.

Pressure-drag reductions greater than those obtained by an axisymmetrical indentation of the fuselage in accordance with the principles of the transonic area rule were obtained at Mach numbers between 1.0 and 1.13 with a configuration having the same longitudinal distribution of area and a localized fuselage shaping in the wing-root juncture in accordance with the natural streamline flow over an infinite sweptback wing. Significant reductions in pressure drag of the basic configuration were also obtained by contouring the fuselage to approximate the

natural streamline flow in the region of the wing-root juncture without regard for the area development.

Langley Aeronautical Laboratory,
National Advisory Committee for Aeronautics,
Langley Field, Va., December 20, 1954.

REFERENCES

1. Whitcomb, Richard T.: A Study of Zero-Lift Drag-Rise Characteristics of Wing-Body Combinations Near the Speed of Sound. NACA RM L52H08, 1952.

2. Harder, Keith C., and Klunker, E. B.: On Slender-Body Theory at Transonic Speeds. NACA RM L54A29a, 1954.

3. Hartley, D. E.: Investigation at High Subsonic Speeds of Wing-Fuselage Intersection Shapes for Sweptback Wings. Part I. Force Measurements on Some Initial Designs. Rep. No. Aero. 2464, British R.A.E., May 1952.

4. Hartley, D. E.: Investigation at High Subsonic Speeds of Wing-Fuselage Intersection Shapes for Sweptback Wings. Part II. Pressure Measurements on Some Initial Designs. Rep. No. Aero. 2503, British R.A.E., Dec. 1953.

5. McDevitt, John B., and Haire, William M.: Investigation at High Subsonic Speeds of a Body-Contouring Method for Alleviating the Adverse Interference at the Root of a Sweptback Wing. NACA RM A54A22, 1954.

6. Boddy, Lee E.: Investigation at High Subsonic Speeds of Methods of Alleviating the Adverse Interference at the Root of a Swept-Back Wing. NACA RM A50E26, 1950.

7. Pepper, William B.: The Effect on Zero-Lift Drag of an Indented Fuselage or a Thickened Wing-Root Modification to a 45° Sweptback Wing-Body Configuration as Determined by Flight Tests at Transonic Speeds. NACA RM L51F15, 1951.

8. Watkins, Charles E.: The Streamline Pattern in the Vicinity of an Oblique Airfoil. NACA TN 1231, 1947.

9. Küchemann, D.: Design of Wing Junction, Fuselage, and Nacelles To Obtain the Full Benefit of Sweptback Wings at High Mach Number. Rep. No. Aero. 2219, British R.A.E., Aug. 1947.

10. Jones, Robert T.: Wing Plan Forms for High-Speed Flight. NACA Rep. 863, 1947. (Supersedes NACA TN 1033.)

11. Jones, Robert T.: Thin Oblique Airfoils at Supersonic Speed. NACA Rep. 851, 1946. (Supersedes NACA TN 1107.)

12. Wright, Ray H., and Ward, Vernon G.: NACA Transonic Wind-Tunnel Test Sections. NACA RM L8J06, 1948.

13. Whitcomb, Richard T., and Fischetti, Thomas L.: Development of a Supersonic Area Rule and an Application to the Design of a Wing-Body Combination Having High Lift-to-Drag Ratios. NACA RM L53H31a, 1953.

TABLE I

DESIGN ORDINATES FOR THE CONFIGURATIONS TESTED

(a) Basic, area-rule-indented, and streamline-contoured bodies.

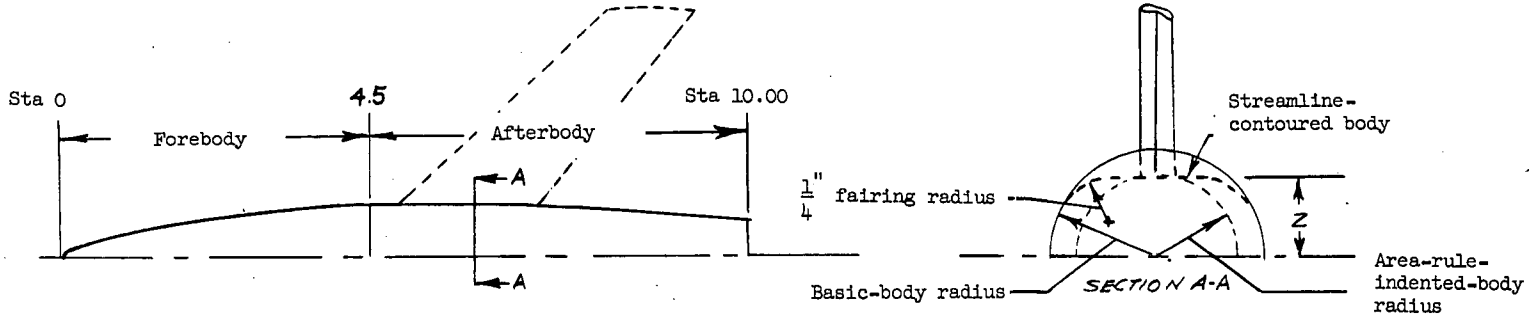

Forebody ordinates	
Station	Radius
0	0
.010	.037
.040	.075
.090	.112
.160	.150
.250	.187
1.000	.375
1.500	.459
2.000	.530
2.500	.620
3.000	.649
3.500	.700
4.000	.740
4.500	.750

Basic-fuselage afterbody ordinates	
Station	Radius
4.500	0.750
4.810	↓
5.135	
5.385	
5.760	
6.385	.750
6.885	.745
7.260	.720
7.510	.700
7.885	.670
8.260	↓
8.635	
9.010	
9.435	
10.000	.510

Area-rule-indented afterbody ordinates	
Station	Radius
4.500	0.750
4.810	.750
5.135	.748
5.385	.738
5.760	.717
6.385	.697
6.885	.682
7.260	.662
7.510	.650
7.885	.623
8.260	.602
8.635	.579
9.010	.565
9.435	.542
10.000	.510

Streamline-contoured afterbody ordinates	
Station	Z
4.500	0.750
5.065	.745
5.185	.735
5.302	.730
5.450	.720
5.570	.710
5.700	.700
5.875	.690
5.955	.680
6.075	.660
6.195	.650
6.375	.645
6.455	.640
6.565	.635
6.695	.635
6.875	.640
6.975	.645
7.275	.670
7.510	.700

TABLE I.- Concluded

DESIGN ORDINATES FOR THE CONFIGURATIONS TESTED

(b) Combination-contoured body

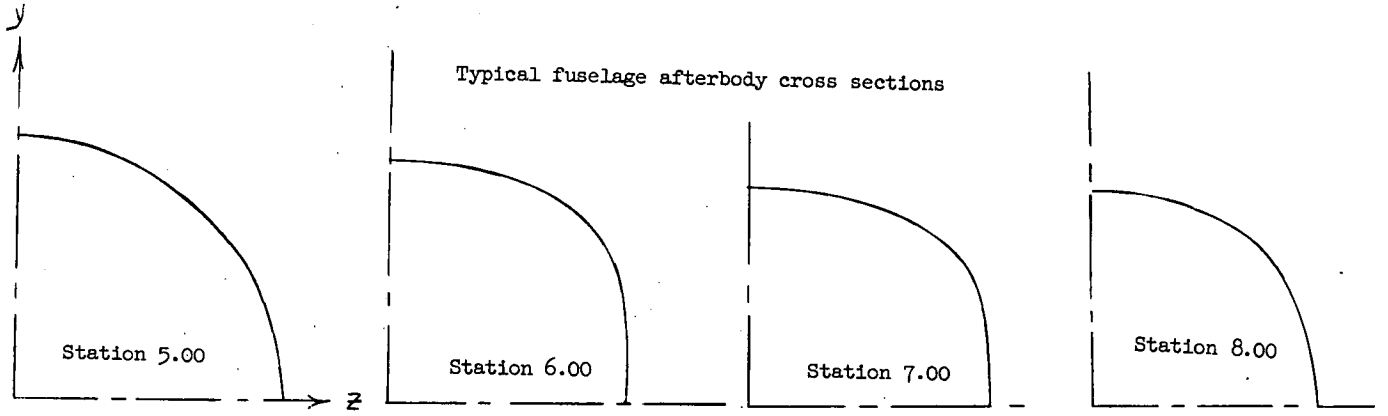

Coordinates for cross-sectional shapes at various fuselage stations

Station 5.0	
z	y
0	0.750
.1	.740
.2	.720
.3	.682
.4	.633
.5	.555
.6	.441
.7	.250
.745	0

Station 6.0	
z	y
0	0.690
.1	.686
.2	.678
.3	.651
.4	.621
.5	.562
.6	.461
.672	0

Station 7.0	
z	y
0	0.618
.1	.615
.2	.603
.3	.587
.4	.556
.5	.501
.6	.420
.645	0

Station 8.0	
z	y
0	0.623
.1	.620
.2	.580
.3	.550
.4	.480
.5	.375
.6	.200
.66	0

Station 9.0	
z	y
0	0.580
.1	.570
.2	.540
.3	.495
.4	.420
.5	.239
.580	0

Station 10.0	
z	y
0	0.510
.1	.500
.2	.468
.3	.410
.4	.318
.5	.107
.510	0

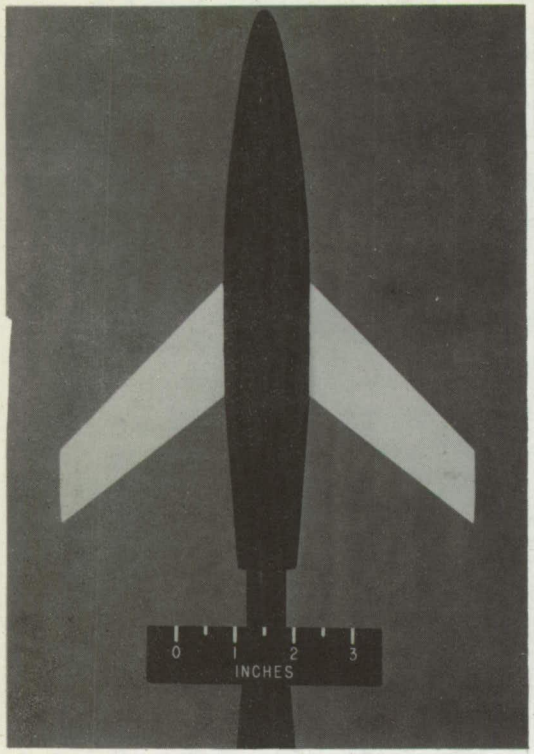

L-84963.1

(a) Basic wing-body configuration.

L-84964.1

(b) Streamline-contoured wing-body configuration.

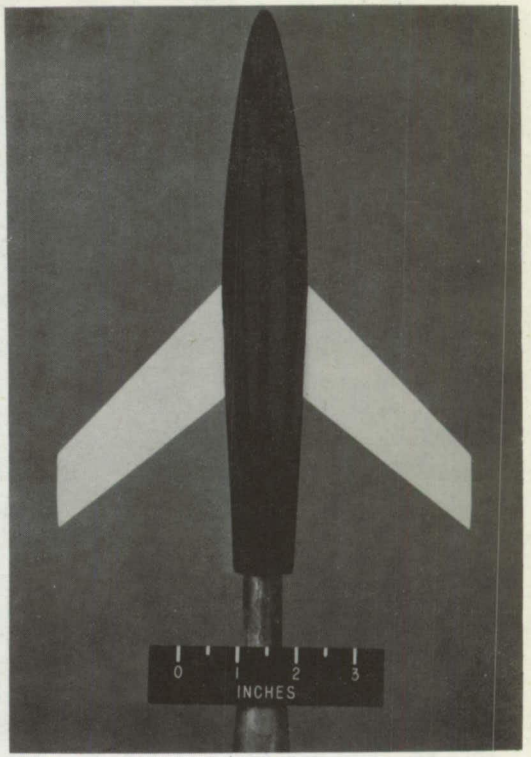

L-84965.1

(c) Area-rule-indented wing-body configuration.

Figure 1.- Photographs of the configurations tested.

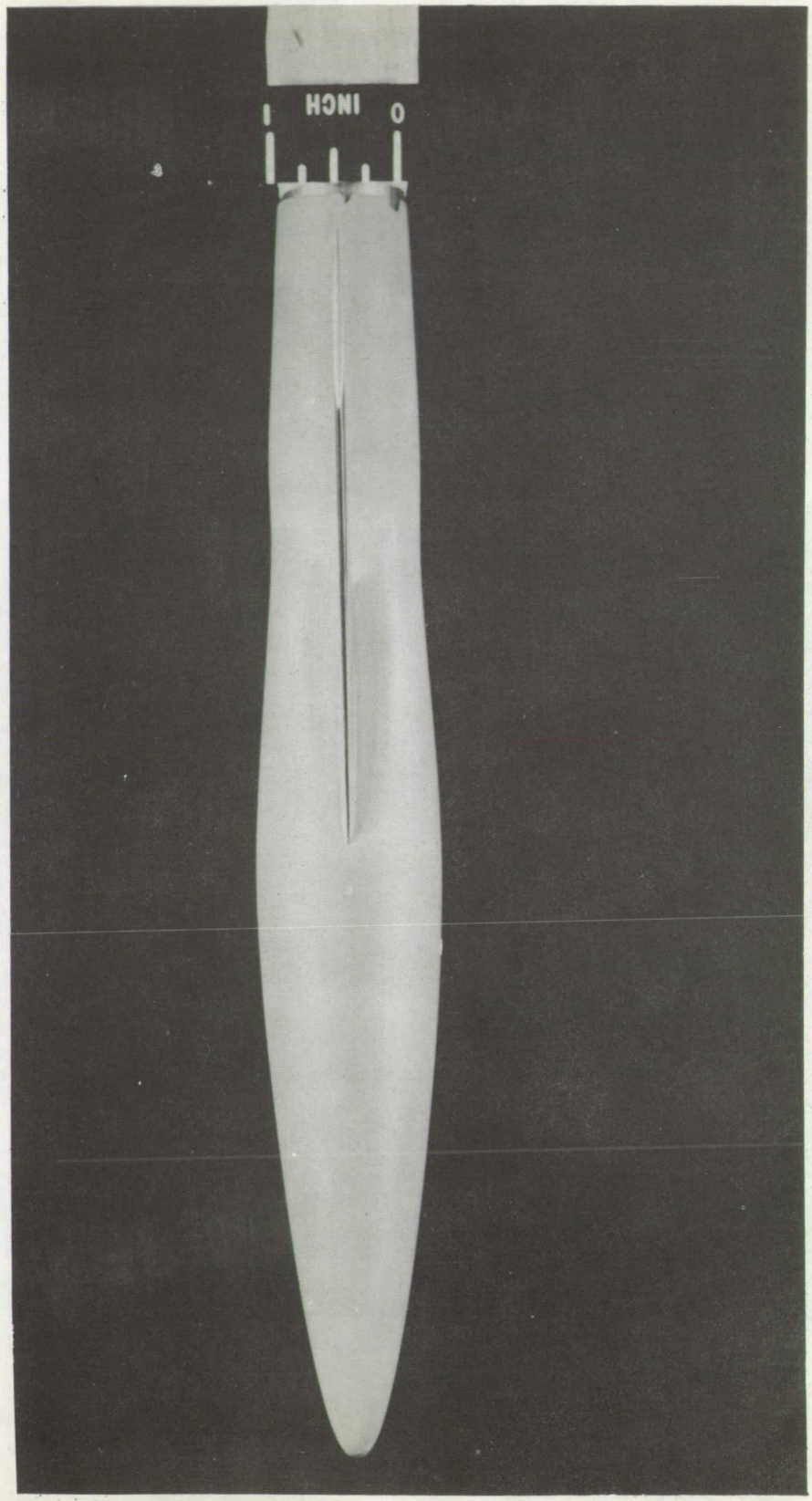

(d) Profile view of combination-contoured wing-body configuration. L-86631

Figure 1.- Continued.

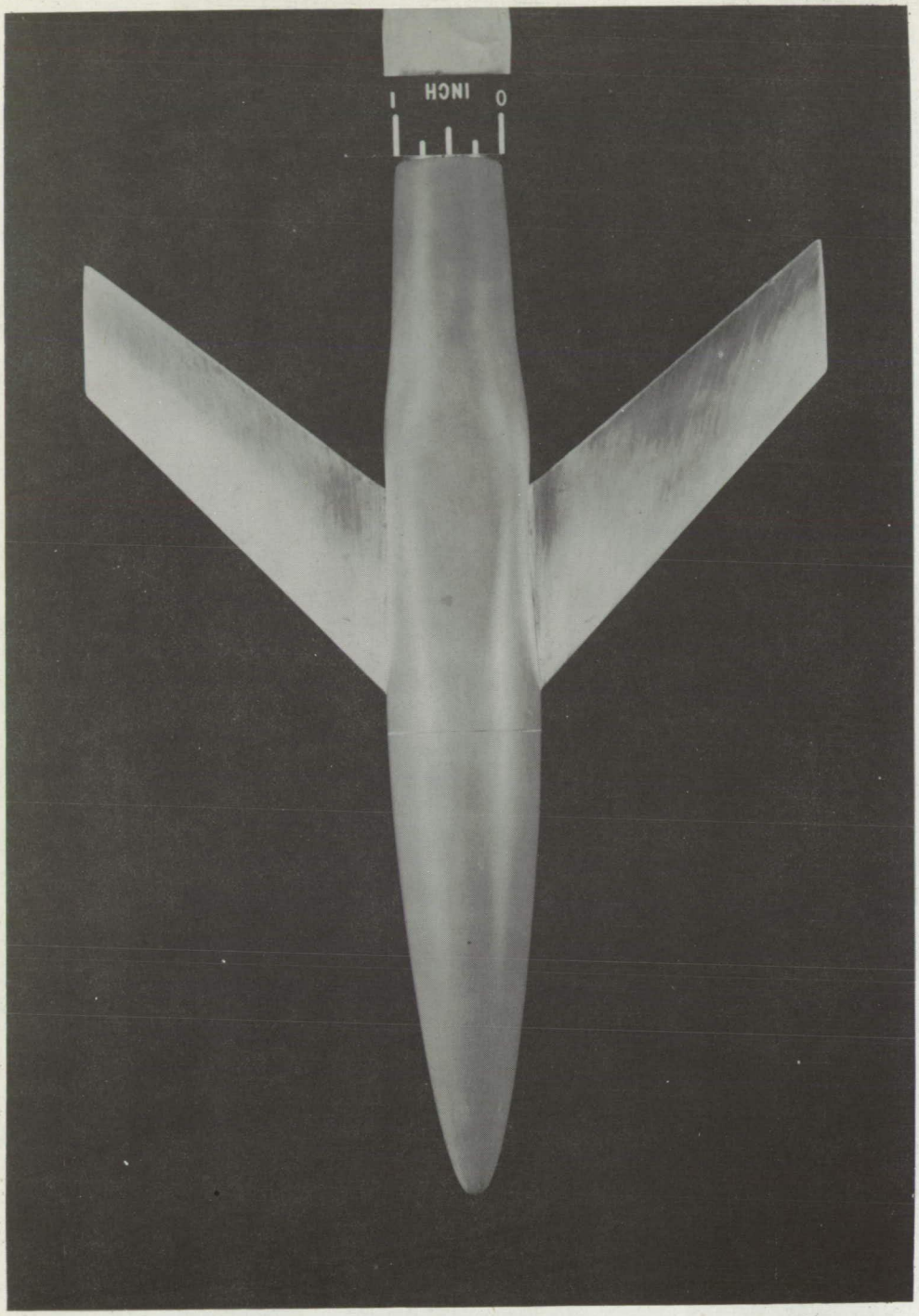

(e) Plan view of combination-contoured wing-body configuration. L-86630

Figure 1.- Continued.

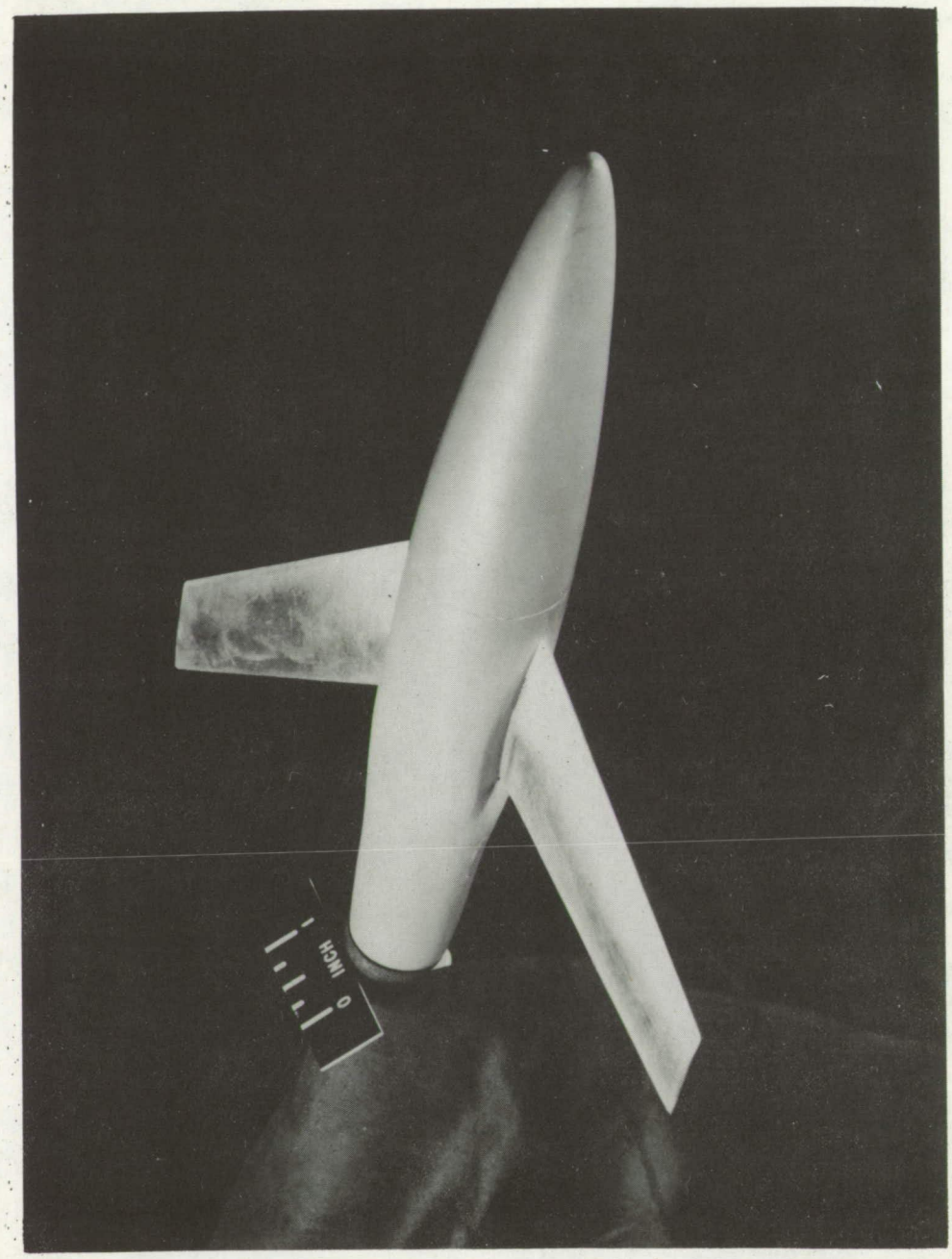

L-86629

(f) Three-quarter view of combination-contoured wing-body configuration.

Figure 1.- Concluded.

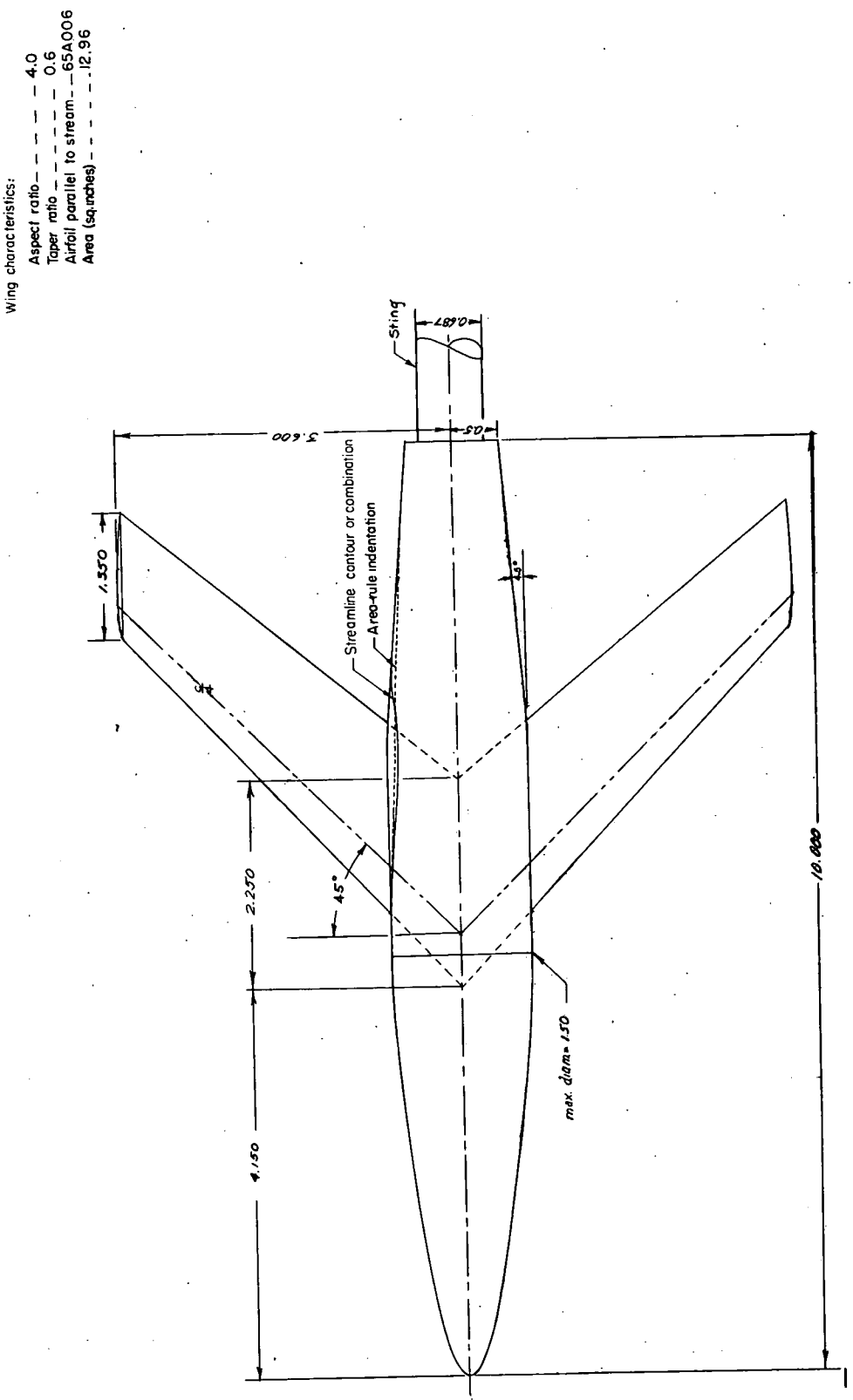

Figure 2.- A diagrammatic sketch of the configurations tested. All dimensions are in inches.

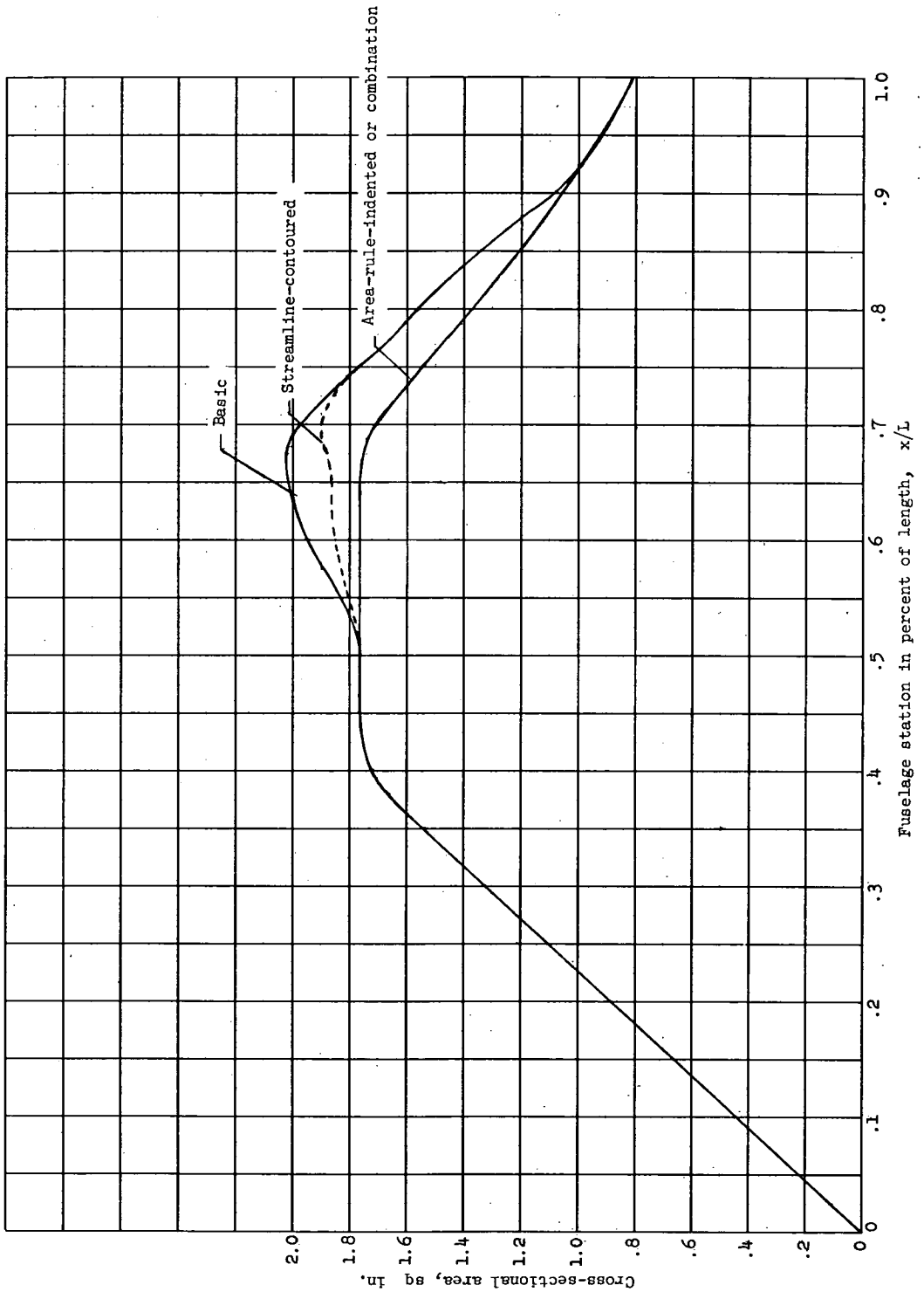

Figure 3.- Longitudinal area development of the wing-body configurations tested.

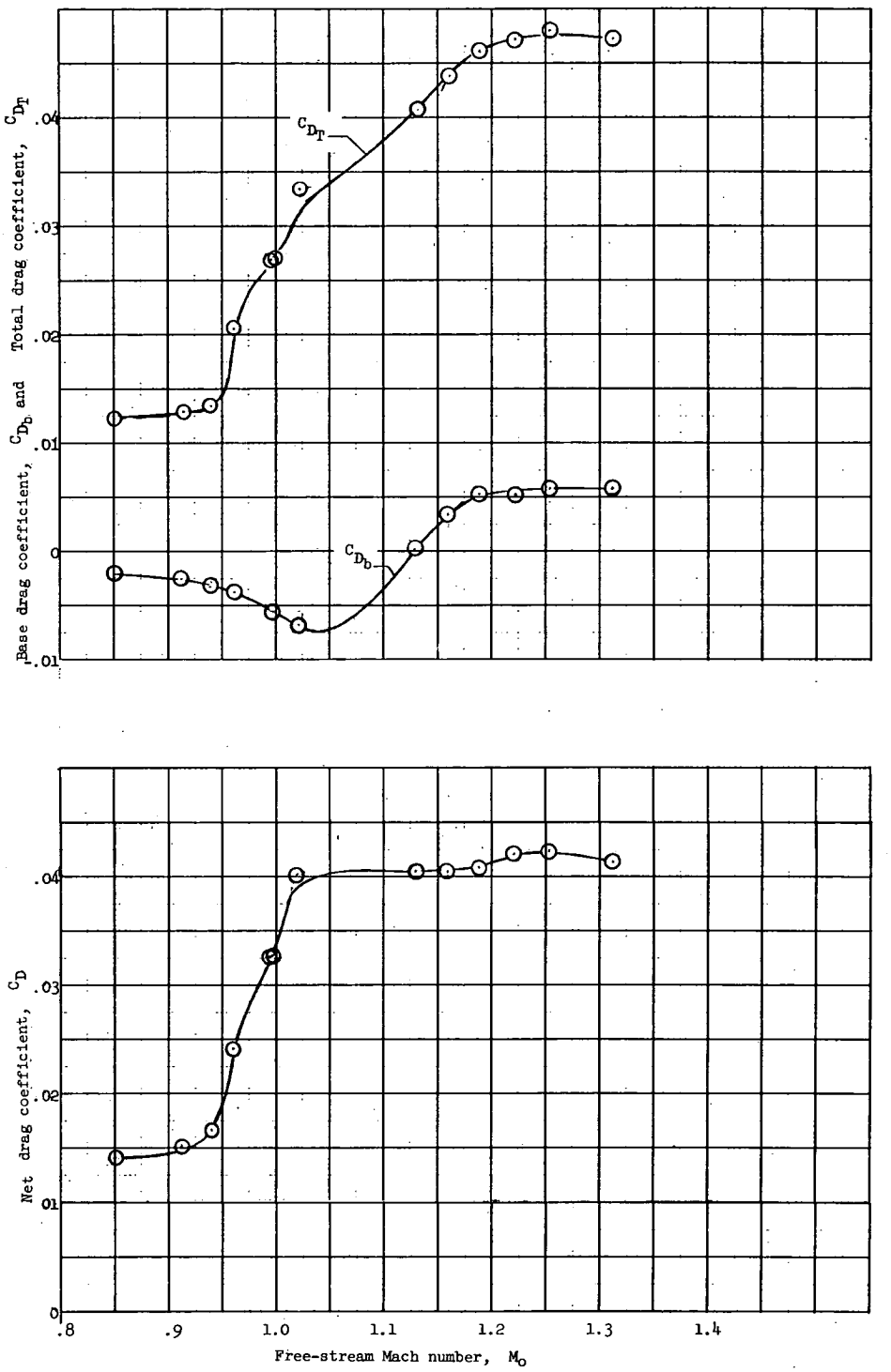

(a) Basic configuration.

Figure 4.- The variation of total, base, and net drag coefficients with Mach number for the four wing-body configurations tested.

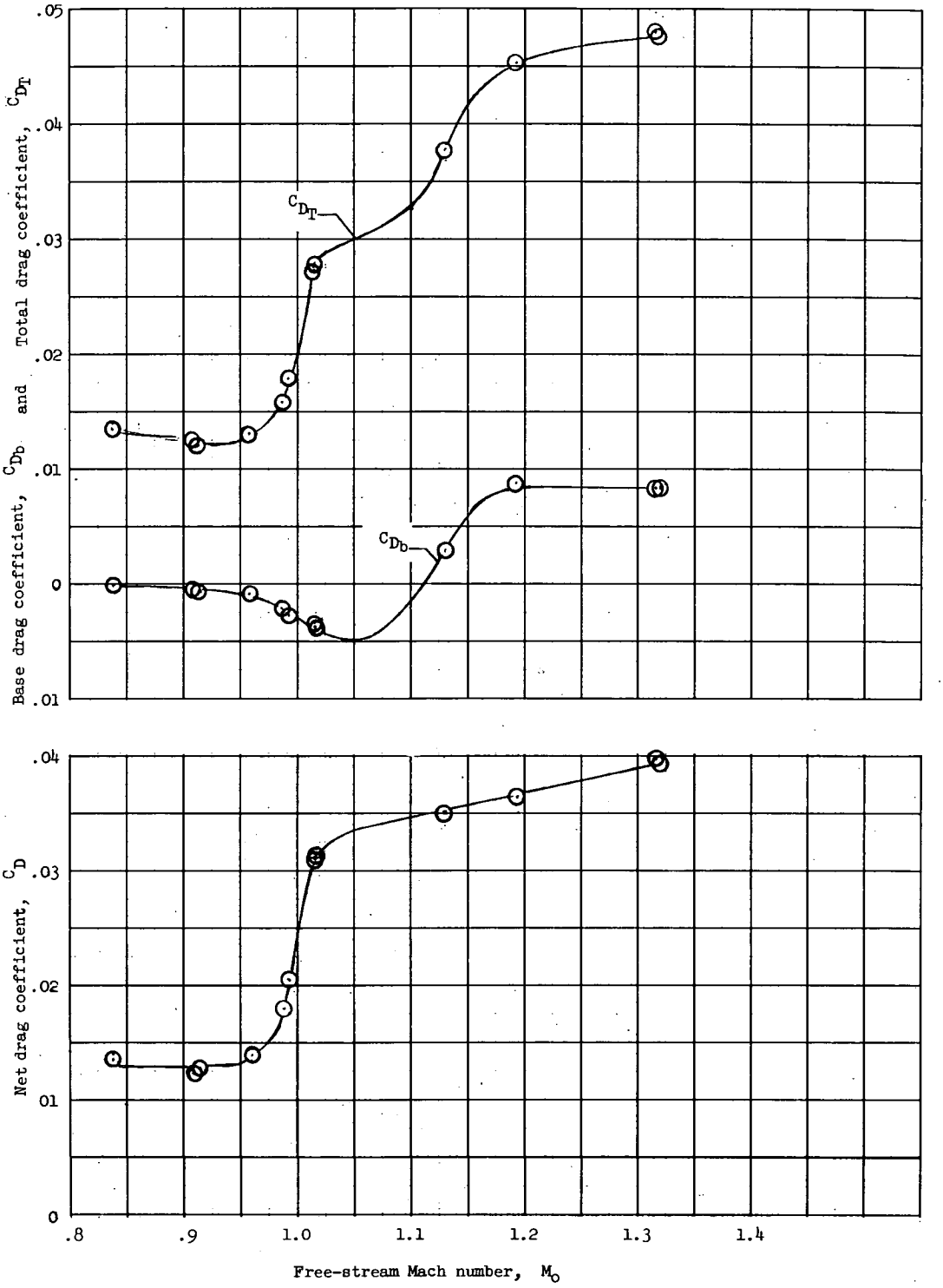

(b) Area-rule-indented configuration.

Figure 4.- Continued.

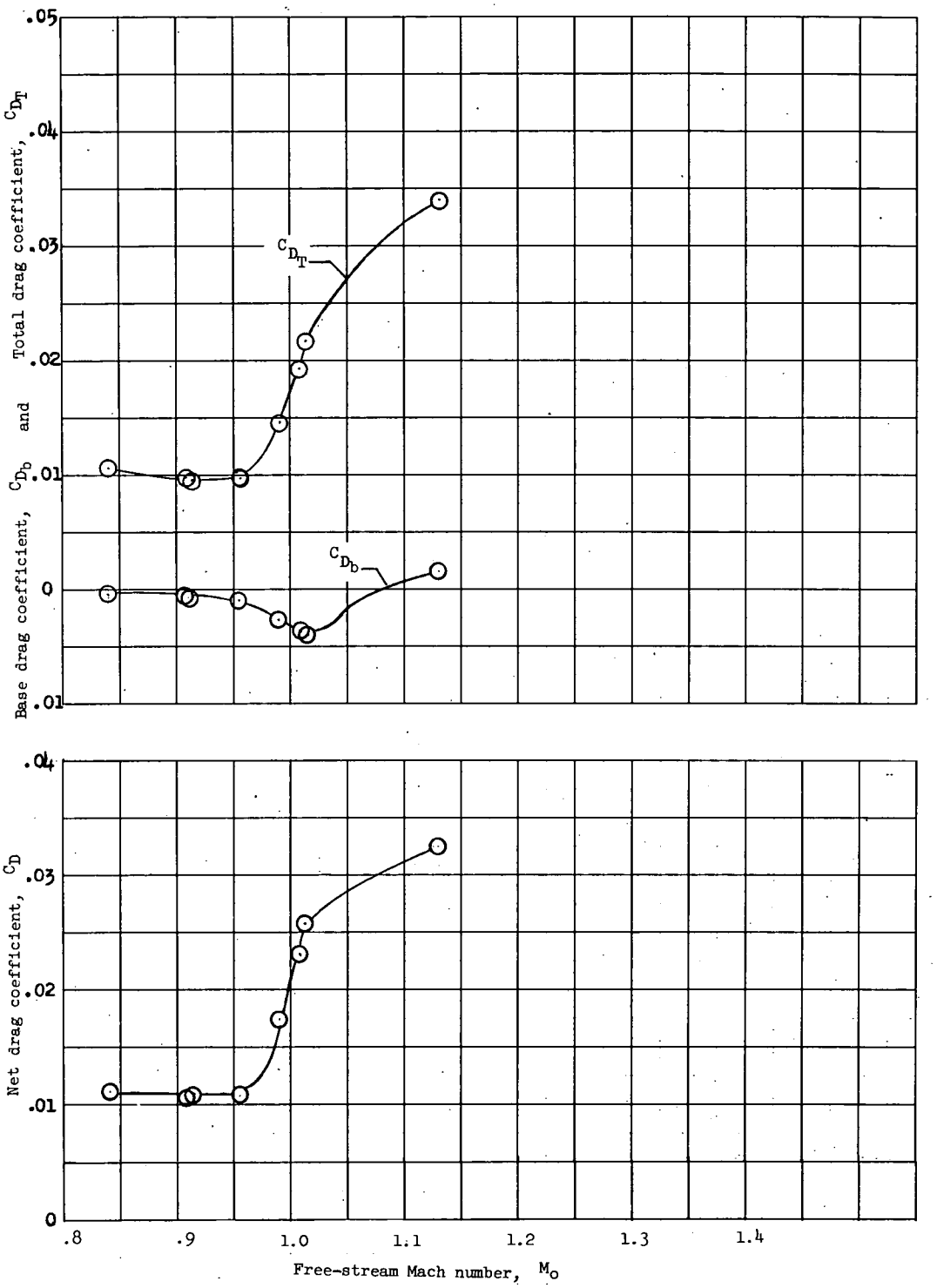

(c) Combination-contoured configuration.

Figure 4.- Continued.

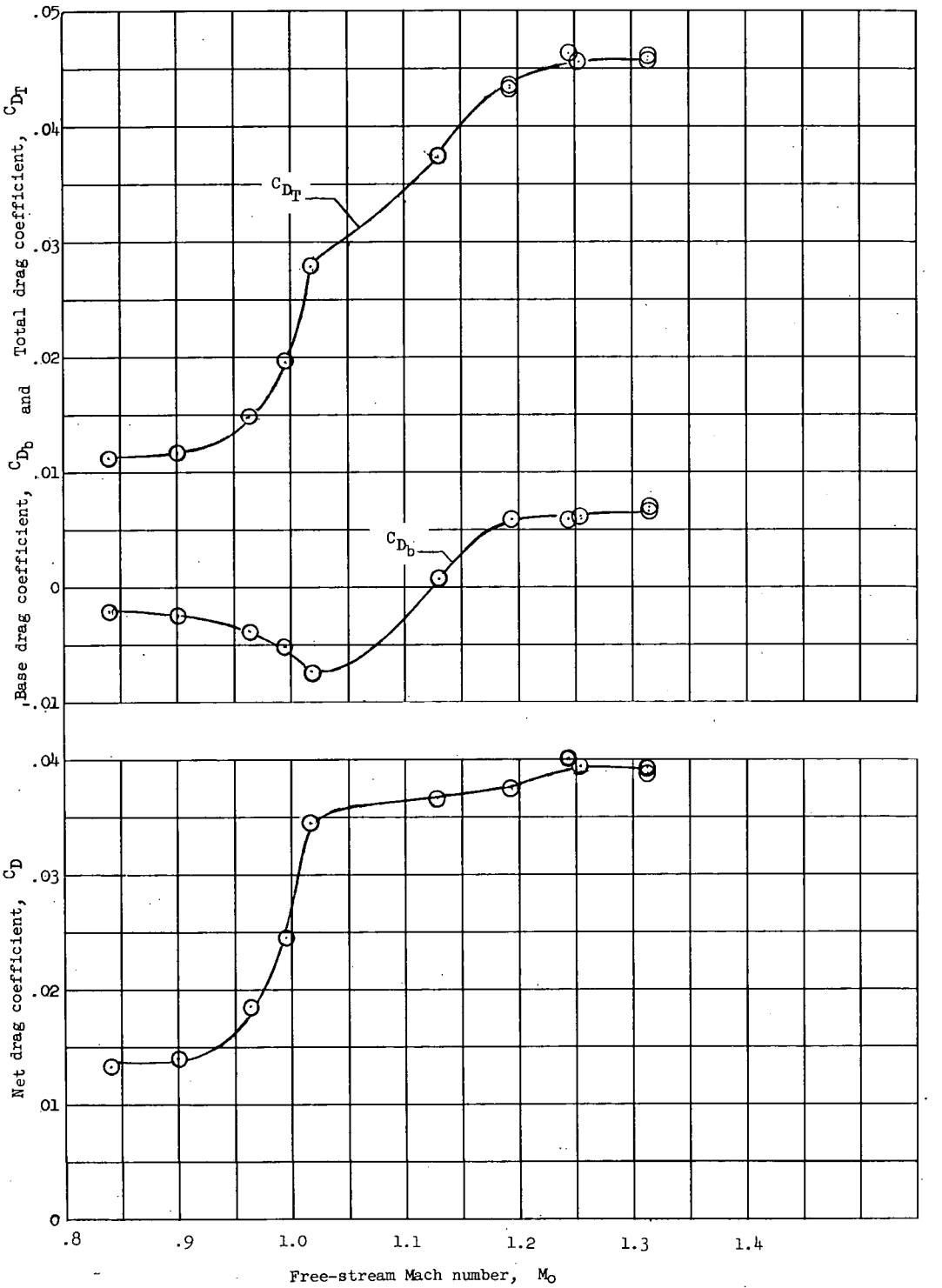

(d) Streamline-contoured configuration.

Figure 4.- Concluded.

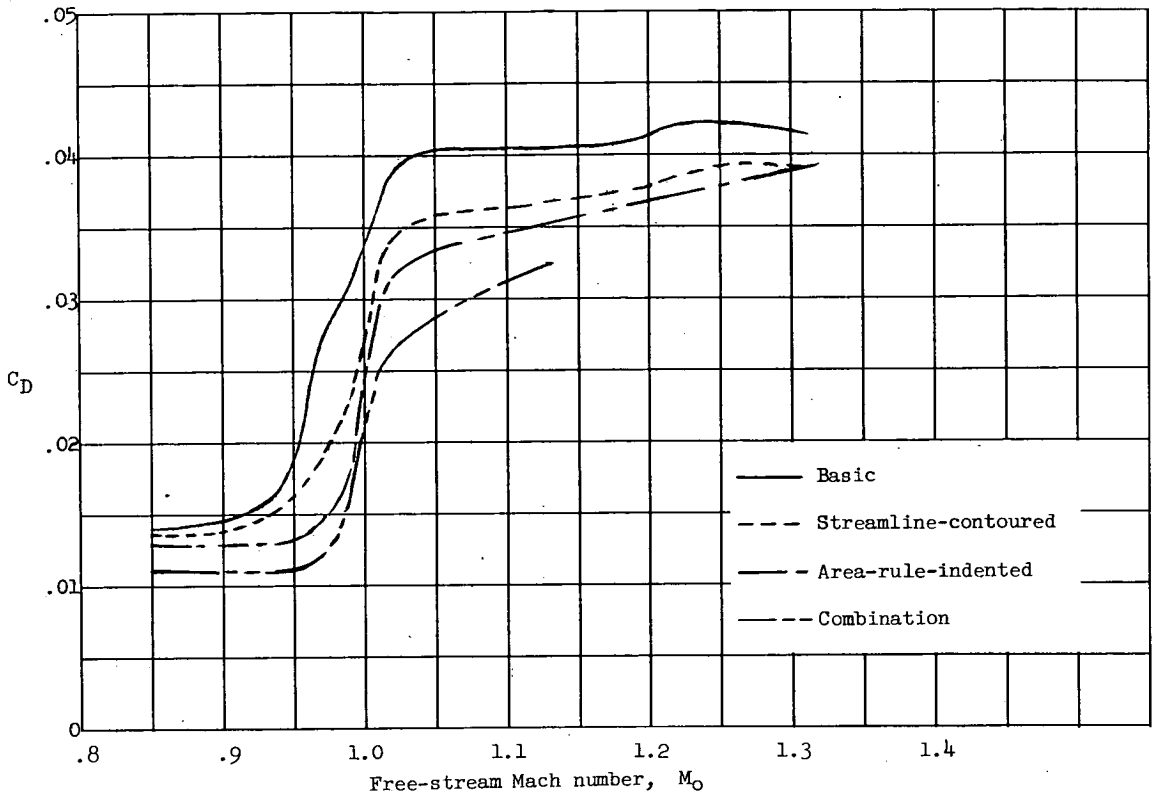

Figure 5.- A comparison of the net-drag-coefficient variation with Mach number for the four wing-body configurations tested.

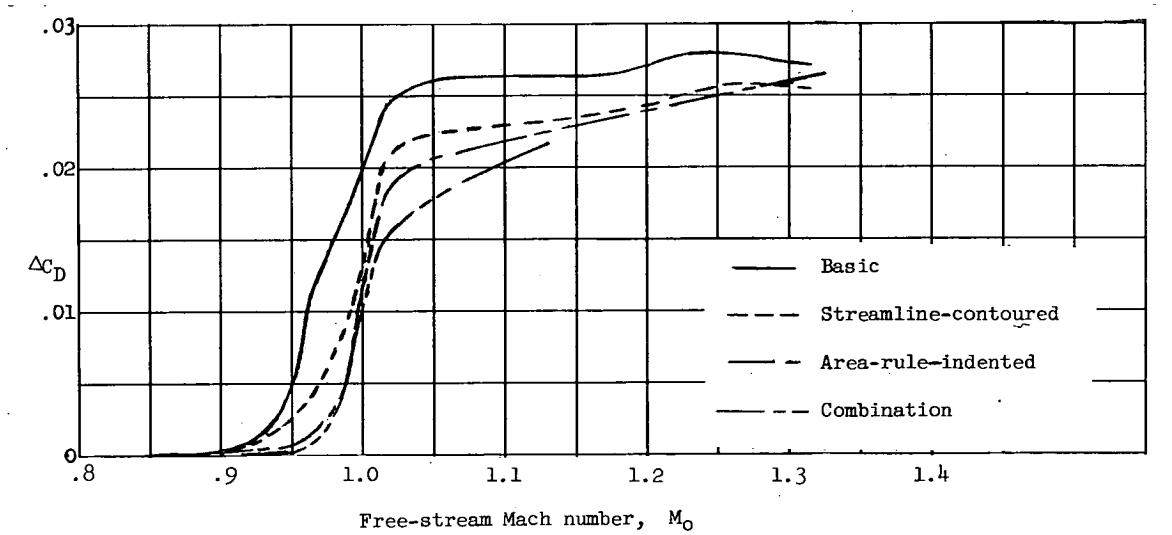

Figure 6.- A comparison of incremental-pressure-drag-coefficient variation with Mach number for the four wing-body configurations tested.